Translational Oncology
www.transonc.com

Volume 9 Number 3 June 2016 pp. 203–210 203

Rapid Cancer Fluorescence Imaging Using A γ-Glutamyltranspeptidase-Specific Probe For Primary Lung Cancer

Haruaki Hino*, Mako Kamiya[†,‡], Kentaro Kitano*, Kazue Mizuno[§], Sayaka Tanaka[†], Nobuhiro Nishiyama[¶], Kazunori Kataoka[§], Yasuteru Urano[†,#,] and Jun Nakajima***

*Department of Thoracic Surgery, The University of Tokyo Graduate School of Medicine, 7-3-1 Hongo, Bunkyo-ku, Tokyo, 113-8655, Japan; [†]Graduate School of Medicine, The University of Tokyo, 7-3-1 Hongo, Bunkyo-ku, Tokyo, 113-0033, Japan; [‡]PRESTO, Japan Science and Technology Agency, K's Gobancho 6F 7, Gobancho, Chiyoda-ku, Tokyo, 102-0076, Japan; [§]Department of Materials Engineering, The University of Tokyo, 7-3-1 Hongo, Bunkyo-ku, Tokyo, 113-8656, Japan; [¶]Tokyo Institute of Technology, Chemical Resources Laboratory, 4259 Nagatsuta Midori-ku Yokohama-shi, Kanagawa, 226-8503, Japan; [#]Graduate School of Pharmaceutical Sciences, The University of Tokyo, 7-3-1 Hongo, Bunkyo-ku, Tokyo, 113-0033, Japan; **CREST, Japan Agency for Medical Research and Development, 1-7-1 Otemachi, Chiyoda-ku, Tokyo, 100-0004, Japan

Abstract

BACKGROUND: We set out to examine the activity of γ-glutamyltranspeptidase (GGT) in lung cancer and the validity of γ-glutamyl hydroxymethyl rhodamine green (gGlu-HMRG) for intraoperative imaging of primary lung cancer. **METHODS**: GGT activities and mRNA expression levels of GGT1 (one of the GGT subtypes) in five human lung cancer cell lines were examined by fluorescence imaging and quantitative reverse transcription polymerase chain reaction. *In vivo* imaging of an orthotopic A549 xenograft model in nude mice was performed to confirm its applicability to intraoperative imaging. Furthermore, *ex vivo* imaging of 73 specimens from lung cancer patients were performed and analyzed to calculate the sensitivity/specificity of gGlu-HMRG for lung cancer diagnosis. **RESULTS**: GGT activities and mRNA expression levels of GGT1 are diverse depending on cell type; A549, H441, and H460 showed relatively high GGT activities and expression levels, whereas H82 and H226 showed lower values. In the *in vivo* mouse model study, tiny pleural dissemination and hilar/mediastinal lymph node metastasis (less than 1 mm in diameter) were clearly detected 15 minutes after topical application of gGlu-HMRG. In the *ex vivo* study of specimens from patients, the sensitivity and specificity of gGlu-HMRG were calculated to be 43.8% (32/73) and 84.9% (62/73), respectively. When limited to female patients, never smokers, and adenocarcinomas, these values were 78.9% (15/19) and 73.7% (14/19), respectively. **CONCLUSIONS**: Although GGT activity of lung cancer cells vary, gGlu-HMRG can serve as an intraoperative imaging tool to detect small foci of lung cancer when such cells have sufficient GGT activity.

Translational Oncology (2016) 9, 203–210

Address all correspondence to: Jun Nakajima, Department of Thoracic Surgery, Graduate School of Medicine, The University of Tokyo 7-3-1 Hongo, Bunkyo-ku, Tokyo, 113-8655, Japan or Yasuteru Urano, Graduate School of Medicine, The University of Tokyo, 7-3-1 Hongo, Bunkyo-ku, Tokyo, 113-0033, Japan.
E-mails: nakajima-tho@h.u-tokyo.ac.jp, uranokun@m.u-tokyo.ac.jp

Received 14 January 2016; Revised 17 March 2016; Accepted 21 March 2016

1936-5233/16
http://dx.doi.org/10.1016/j.tranon.2016.03.007

Introduction

Lung cancer has become the leading cause of cancer-related death in many countries, including Japan [1]. Even when state-of-the-art diagnostic tools are used, it is challenging to detect and visualize minute lung cancer cells, especially those only a few millimeters in diameter. Recently, we reported an activatable fluorescence probe, γ-glutamyl hydroxymethyl rhodamine green (gGlu-HMRG), which can be used as an intraoperative imaging tool for visualizing cancers less than 1 mm in diameter [2]. gGlu-HMRG is nonfluorescent but can be converted to highly fluorescent hydroxymethyl rhodamine green (HMRG) upon reaction with γ-glutamyltranspeptidase (GGT). GGT has essential roles in glutathione and drug metabolism, as well as in leukotriene catabolism, which is localized mainly to the surface of living cells [3] and which is highly expressed in some normal tissues such as the proximal tubules of the kidney and the hepatic bile epithelium [4]. GGT is also involved in anticancer drug resistance in cancer cells and acceleration of tumor proliferation including a relation with the ras oncogene [4–8], and is highly expressed in malignant ovarian tumor, breast cancer, carcinoma of the thyroid, and lung cancer [9–11]. Therefore, in this study, we firstly investigated the feasibility of gGlu-HMRG as an intraoperative diagnostic tool for primary lung cancer.

Material and Methods

Activatable Fluorescence probe

gGlu-HMRG was used as an activatable fluorescence probe targeting GGT [2]. A 10-mM DMSO stock solution of gGlu-HMRG was prepared and diluted to the final concentration described in the experimental section.

Cell Lines and Culture Conditions

A549 was purchased from Riken Cell Bank, and four human lung cancer cell lines (H441, H460, H82, and H226) were purchased from the American Type Culture Collection. A549 cells were cultured in high-glucose Dulbecco's modified Eagle's medium (Wako, #04429765) supplemented with 10% fetal bovine serum (Gibco, #10437028) and 1% penicillin-streptomycin (Gibco, #15070063), and H441, H460, H82, and H226 cells were cultured in RPMI-1640 medium (Gibco, #11875093) supplemented with 10% fetal bovine serum (Gibco, #10437028) and 1% penicillin-streptomycin (Gibco, #15070063) at 37°C in a humidified incubator with 5% CO_2.

Cell Lysate

Cell lysates of each cell line were prepared using CelLytic M (Sigma-Aldrich, #2978) according to the manufacturer's instructions. Lysate protein concentration was calculated by the Bradford assay.

RNA Interference

The lung cancer cell lines (A549, H460, H441, H82, and H226) were transfected with 10 nM of GGT1 siRNA (siRNA1 and siRNA2) designed to interfere with GGT1 mRNA expression or control siRNA using Lipofectamine RNAiMAX transfection reagent (Invitrogen, #13778030). GGT1 is one of the subtypes of GGT, and the sequence of each siRNA was as follows: GGT1 siRNA1 sense: 5′-rCrArArCrArGrCrArCrCrArCrArCrGrArArArArGrC-3′, GGT1 siRNA1 antisense: 5′-UUUUrCrGUrGUrGrGUrGrGUrGUUrGUrA-3′, GGT1 siRNA2 sense: 5′-rCrCrArArGrGrArArArCrCUrGrACAACCATG-3′, GGT1 siRNA2 antisense: 5′-TGGTTGUrCrArGrGUUrCrCUUrGrGrArG-3′, control siRNA sense: 5′-rGUrArCrCrGrCrArCrGUrCrAUUrCrGUrAUrC-3′, control siRNA antisense: 5′-UrArCrGrArArAUrGrArCrGUrGrCrGrGUrArCrGU-3′. Transfected cells were cultured for 2 days in an 8-well chamber slide (ibidi, #ib80826) or a 10-cm dish and subsequently used for live-cell fluorescence imaging or quantitative reverse transcription polymerase chain reaction (qRT-PCR) analysis, respectively.

qRT-PCR analysis

Total mRNA of the lung cancer cell lines (A549, H460, H441, H82, and H226) was extracted using TRIzol RNA Isolation Reagent (Gibco, #10296028), and first-strand cDNAs were synthesized using the PrimeScript II 1st strand cDNA Synthesis Kit (TAKARA, #C6210A). qRT-PCR was performed with Light Cycler 480 System II (Roche) in triplicate using a LightCycler 480 SYBR Green I Master (Roche, #04707516001). Cycling conditions were as follows: 50°C for 2 minutes, 95°C for 10 minutes, followed by 40 cycles of 95°C for 15 seconds, 60°C for 1 minute, and 72°C for 1 minute. The GGT1 mRNA expression level of each lung cancer cell line was measured and normalized to HPRT1 mRNA expression level. The primer sequences used were as follows: GGT1, forward: 5′-GTGTTCTGCCGGGATAGAAA-3′; GGT1, reverse: 5′-CAGGTCCTCAGCTGTCACAA-3′; hHPRT1, forward: 5′-GTTCTTTGCTGACCTGCTGGAT-3′; hHPRT1, reverse: 5′-CTTTTATGTCCCCCGTTGACTG-3′.

Animals

Female severe combined immunodeficiency disease mice (BALB/cAjcl-nu/nu) were purchased from CLEA Japan, Inc. These mice had been raised from birth in a specific pathogen-free environment. The mice were 7 weeks old and weighed 20-25 g when the experiments started.

An orthotopic A549 xenograft model was developed in nude mice as follows [12,13]: A549 cells were harvested and suspended (4×10^7 cells/ml) in PBS (–) and mixed with the same volume of 10% Matrigel. BALB/cAjcl-nu/nu mice were anesthetized by intraabdominal injection of ketamine (2 mg/mouse) and xylazine (0.2 mg/mouse), and a small skin incision, approximately 2 cm on the left chest wall, was made. A total of 25 μl of the above-mentioned cell suspension was directly injected into left lung with a 30-gauge needle attached to a 1-ml syringe. The skin incision was closed with 4-0 nylon and observed until mice woke up from the anesthesia. After 1-2 weeks of breeding, mice were sacrificed and evaluated by the fluorescence imaging system. A total of 19 mice were used for *in vivo* imaging. All animal studies were approved by Office for Life Science Research Ethics and Safety, The University of Tokyo.

In Vitro Fluorescence Imaging Study

Cultured in 8-well chamber slides (ibidi, #ib80826), fluorescence images were captured before and 5, 10, and 30 minutes after probe application (1 μM solution of gGlu-HMRG in Dulbecco's modified Eagle's medium or RPMI) by confocal fluorescence microscopy SP5 (Leica Microsystems) at 37°C. The excitation and emission wavelength was 488 nm and 500-600 nm, respectively.

Lung cancer cell lysates were mixed with 5.5 μM gGlu-HMRG with PBS (–) in a 96-well plate. The fluorescence intensity was measured in triplicate before and 5, 10, 15, 20, 25, and 30 minutes after lysate addition on an SH-8000 plate reader (Corona Electric). The fluorescence intensity was standardized by lysate protein concentration.

In Vivo Fluorescence Imaging Study of Mice

A 10-μM solution of gGlu-HMRG in PBS (–) was topically dripped into the left thoracic cavity of the orthotopic A549 xenograft

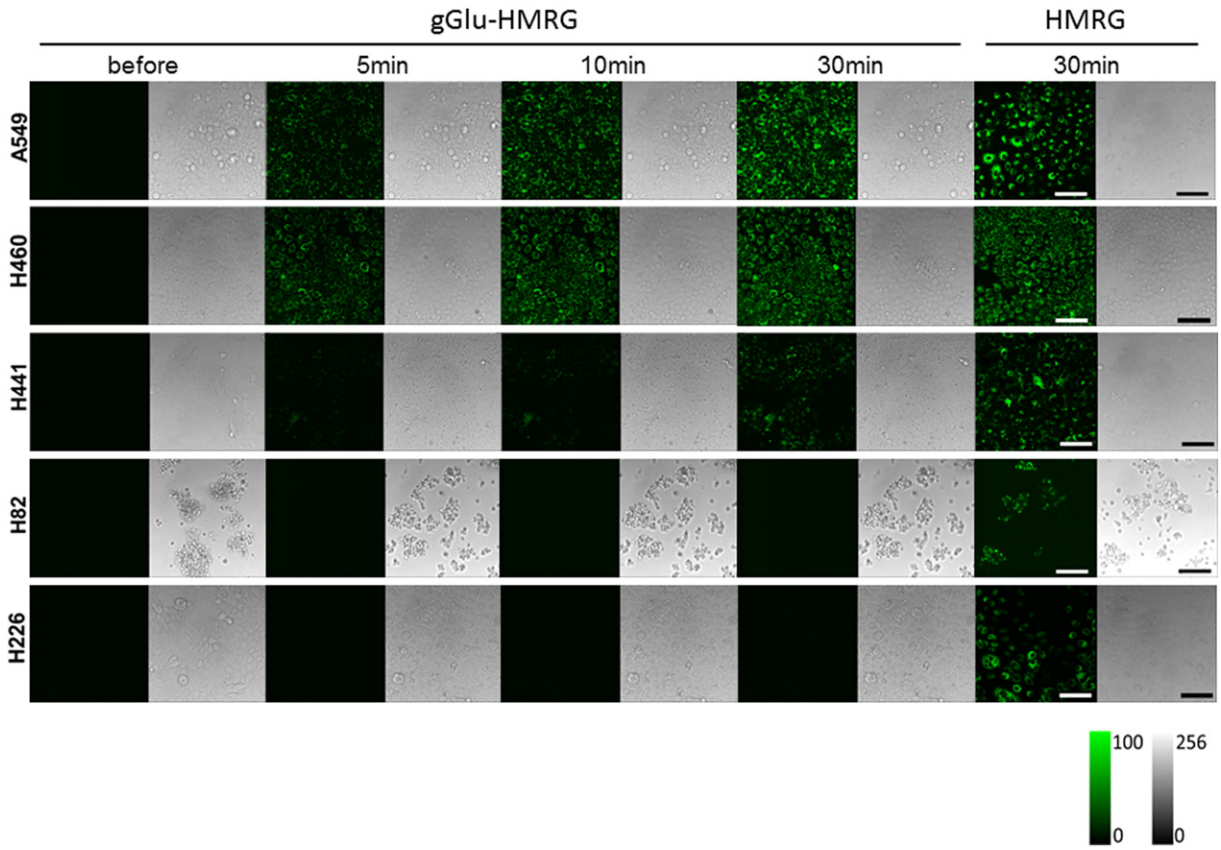

Figure 1. Confocal fluorescence imaging of lung cancer cell lines loaded with 1 μM gGlu-HMRG. Images were captured before and 5, 10, and 30 minutes after probe application. Images of cells loaded with 1 μM HMRG were captured after 30 minutes, serving as positive controls. Strong fluorescence signals were observed after 30 minutes from A549, H460, and H441 cells, but not from H82 and H226 cells. Scale bar represents 100 μm.

model. After approximately 15 minutes, white light and fluorescence images were captured by fluorescence stereo microscopy (Leica M 165FC, Leica Microsystems) at room temperature. Excitation and emission filters were 460-500 nm band pass and 510 nm long pass, respectively.

Ex Vivo Fluorescence Imaging Study of Patient Specimens

A total of 73 specimens, including lung tumor and normal lung, were obtained from the Department of Thoracic Surgery, Graduate School of Medicine, The University of Tokyo (e-Table 1). All the

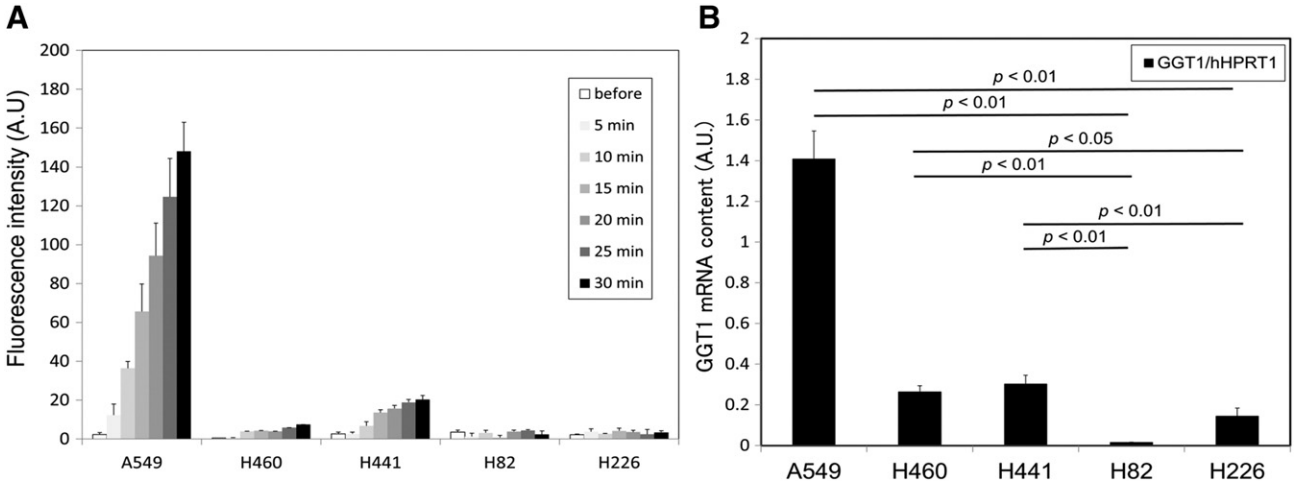

Figure 2. Lysate assay and qRT-PCR of lung cancer cell lines. (A) Fluorescence intensity of lung cancer cell lysate before and 1, 5, 10, 20, and 30 minutes after application of 5.5 μM gGlu-HMRG. Fluorescence intensity increased gradually in the lysates of A549, H460, and H441, but not in H82 and H226. Bar represents fluorescence intensity (A.U.) + standard deviation. (B) Relative GGT1 mRNA expression levels of five lung cancer cell lines measured by qRT-PCR. hHPRT1 was used as a reference gene. A549, H460, and H441 had significantly higher relative GGT1 expression compared with that of H82 and H226 (P < .05-.01). Bar represents the relative GGT1 mRNA contents (A.U.) + standard deviation.

patients were provided written informed consent for this *ex vivo* lung cancer fluorescence imaging study and the review of their medical charts. The Research Review Board at our institution examined and approved the research protocol in accordance with the Declaration of Helsinki. Tumor stage was determined according to the seventh edition of the TNM staging system of the International Union Against Cancer, and histologic tumor type was assessed according to the third edition of the World Health Organization classification [14,15]. All gGlu-HMRG fluorescence imaging studies were performed within 1-2 hours after lung resection. Images were captured by Maestro *in vivo* imaging system (CRi Inc.) before and 5, 10, and 30 minutes after applying approximately 100 μl of 50 μM gGlu-HMRG solution in PBS (–) to lung tumor and normal lung specimens, respectively, at room temperature. The excitation and emission wavelength was 445-490 nm and 515 nm long pass, respectively. Regions of interest were drawn three times for both lung tumor and normal lung, and the mean fluorescence intensity was calculated using Maestro software. Increase in fluorescence intensity was defined by subtracting initial fluorescence intensity from that measured after 30 minutes of incubation with the probe. After the imaging experiment, specimens were preserved in 10% formalin for hematoxylin and eosin staining.

Statistical Analysis

Statistical analysis was performed using JMP 11.0 pro (SAS Institute Inc.). Sensitivity, specificity, positive predictive value (PPV), negative predictive value (NPV), accuracy, and false-positive and -negative rates

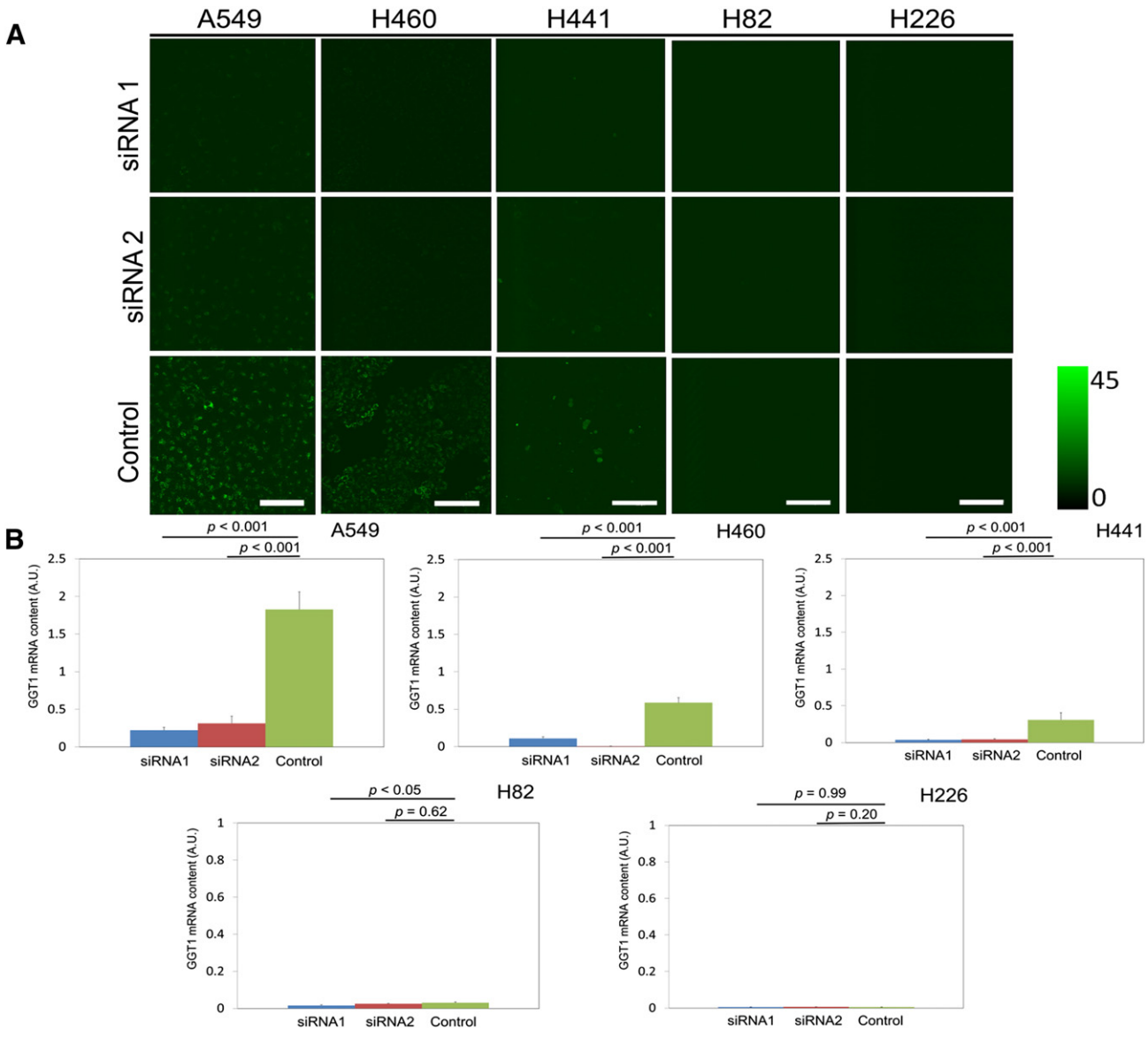

Figure 3. RNA interference targeted to GGT1. (A) Confocal fluorescence imaging of lung cancer cell lines. Cells were transfected with GGT1 siRNA (siRNA 1 and siRNA 2) or control siRNA, followed by incubation with 1 μM gGlu-HMRG for 30 minutes. Scale bar represents 100 μm. (B) Relative GGT1 mRNA expression level of lung cancer cell lines transfected with GGT1 siRNA (siRNA1 and siRNA2) or control siRNA measured by qRT-PCR. hHPRT1 was used as a reference gene. GGT1 mRNA contents of A549, H460, and H441 transfected with siRNA 1 and siRNA2 were significantly suppressed compared with those transfected with control siRNA respectively ($P < .001$-$.05$). In contrast, there was no significant difference in GGT1 mRNA contents of H82 and H226 ($P < .05$, $P = .20$-$.99$). Bar represents relative GGT1 mRNA contents (A.U.) + standard deviation.

were calculated by receiver operating characteristic curves, and chi-square tests and Student's *t* tests were performed where applicable and relevant. Differences were considered statistically significant when the probability (*P*) value was < .05.

Results

In Vitro and In Cellulo Studies of GGT1 Activity

Live-cell fluorescence imaging using confocal fluorescence microscopy revealed that the lung cancer cell lines had different GGT activity. After incubating with 1 μM gGlu-HMRG solution, we observed a strong fluorescence signal from A549, H460, and H441 cells in several minutes, but not from H82 and H226 cells (Figure 1). The lysate assay also demonstrated differences in GGT activity among lung cancer cell lines, giving almost identical results as those obtained through live-cell fluorescence imaging (Figure 2*A*). By qRT-PCR analysis, the relative GGT1 mRNA expression levels of A549, H460, and H441 were significantly higher to those of H82 and H226 ($P < .05$-$.01$) (Figure 2*B*). Among several GGT subtypes, we focused on GGT1 because this subtype is reported to be involved in both glutathione catabolism and anticancer drug resistance, which was characterized by cancer cell [3].

RNA Interference Experiments Targeted to GGT1

In A549, H460, and H441 cells, we observed significantly reduced fluorescence signal when cells were pretransfected with GGT1 siRNAs compared with those transfected with control siRNA. In contrast, in H82 and H226 cells, there was no significant difference in fluorescence signal intensity whether cells were transfected with GGT1 siRNAs or control siRNA (Figure 3*A*). We also confirmed that the relative GGT1 mRNA expression levels of A549, H460, and H441 cells transfected with GGT1 siRNAs were significantly suppressed compared with those transfected with control siRNA ($P < .001$), whereas those of H82 and H226 cells transfected with GGT1 siRNAs were as low as those transfected with control siRNA by qRT-PCR analysis ($P < .05$, $P = 0.20$–0.99) (Figure 3*B*).

In Vivo Imaging of the Orthotopic A549 Xenograft Model

Using white light imaging, it was difficult to recognize the minute pleural dissemination and lymph node metastases, which were less than 2-3 mm in diameter. However, these lesions were clearly visualized 15 minutes after topical dripping of gGlu-HMRG (Figure 4, *A*–*C*). Aggregation of A549 was ascertained by hematoxylin and eosin staining of extracts from lung tumor, hilar and mediastinal lymph nodes, and pleural dissemination, respectively (Figure 4, *D*–*F*).

Ex Vivo Imaging of Specimens from Lung Cancer Patients

In cases 1 and 2, we observed a gradual increase in fluorescence in the lung tumor region compared with that in normal lung after topical application of 50 μM gGlu-HMRG. We also confirmed increasing fluorescence signal over 30 minutes, evidenced by data from the intensity graph. In contrast, in case 3, the fluorescence intensity in lung tumor and normal lung did not change much even after 30 minutes post probe application (Figure 5, *A* and *B*). Cases 1 and 2 were confirmed histologically as adenocarcinoma, and case 3 was identified as squamous cell carcinoma. Analyzed by receiver operating characteristic curves, the sensitivity and specificity of fluorescence imaging for lung cancer were calculated to be 43.8% (32/73) and 84.9% (62/73), respectively, and PPV, NPV, and accuracy were 74.4% (32/43), 60.2% (62/103), and 64.4% (94/146), respectively (Figure 6, *A* and *B*). The false-positive and -negative rates were 15.1% (11/73) and 56.2% (41/73), respectively. On the basis of clinicopathological analysis, cancer in females, never smokers, and cases of adenocarcinomas were detected more often by fluorescence imaging ($P < .001$-$.05$) (e-Figure 1). When limiting

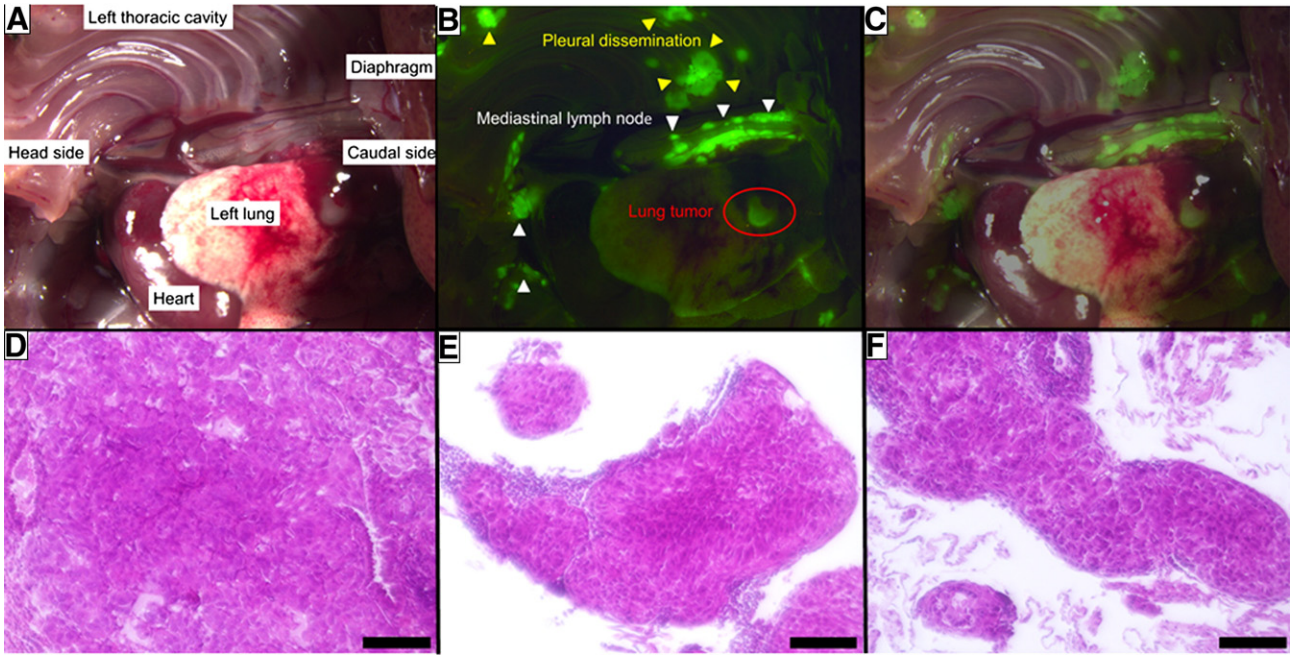

Figure 4. White light and fluorescence images of hilar and mediastinal lymph node metastasis and pleural dissemination in a murine orthotopic A549 xenograft model, captured by stereo fluorescence microscopy. Every lesion with strong fluorescence was pathologically confirmed to be an aggregation of A549 lung cancer cells by hematoxylin and eosin staining. (A) White light image. (B) Fluorescence image. (C) Merged image of white light and fluorescence. (D) Hematoxylin and eosin–stained lung tumor. (E) Hematoxylin and eosin staining of mediastinal lymph node. (F) Hematoxylin and eosin staining of pleural dissemination. Scale bar represents 100 μm.

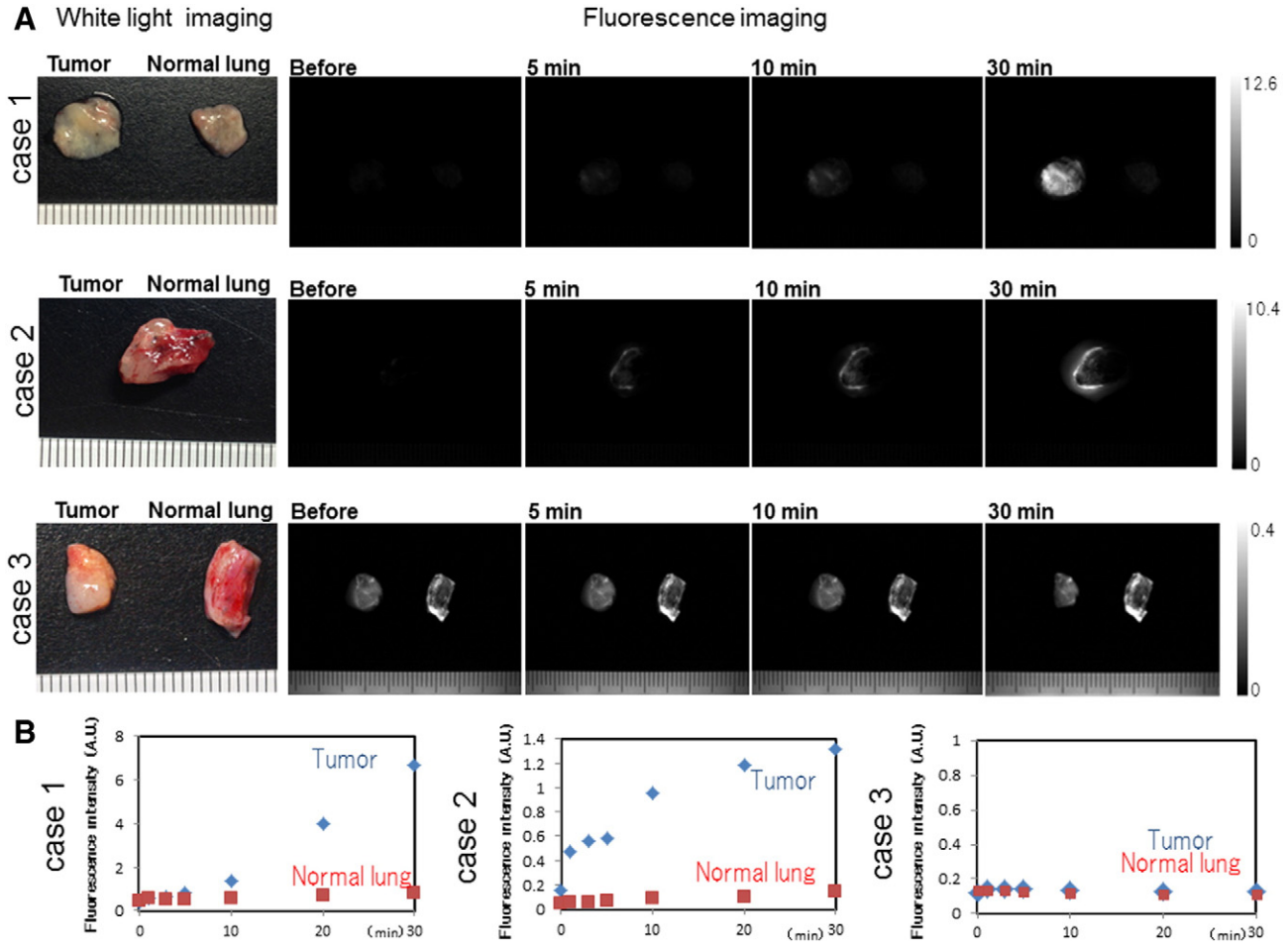

Figure 5. *Ex vivo* fluorescence imaging of specimens from lung cancer patients. (A) White light and fluorescence images of lung cancer specimens. A total of 50 μM gGlu-HMRG was applied to lung tumor and normal lung tissue, and images were captured before and 5, 10, and 30 minutes after by Maestro with appropriate exposure time. Fluorescence image at 540 nm was extracted. Fluorescence intensity of the lung tumor was increasing in case 1 and 2, but not in case 3. (B) Fluorescence intensity values of lung tumor and normal lung in case 1, 2, and 3 were calculated. Fluorescence intensity gradually increased in case 1 and 2, but not in case 3.

the data set to cancer in females, never smokers, and cases of adenocarcinomas (N = 19), the sensitivity and specificity were 78.9% (15/19) and 73.7% (14/19), respectively, and PPV, NPV, and accuracy were 78.9% (15/19), 73.7% (14/19), and 76.3% (29/38), respectively (Figure 6, *C* and *D*). The false-positive and -negative rates were 26.3% (5/19) and 21.1% (4/19), respectively.

Discussion

Lung cancer has become a leading cause of cancer-related death in Japan [1]. To improve prognosis, many efforts have been made to develop effective intraoperative diagnostic tools to visualize cancer cells with high sensitivity [16]. For example, Zhang et al. reported that the COX-2-specific fluorescence probe, ANQ-IMC-6, could visualize cancer cells at the early stage [17]. Koyama et al. demonstrated that an optical probe conjugated to HER2 antibody enabled detection of pulmonary metastasis in *in vivo* imaging [18]. Clinically, five-aminolaevulinic acid has been widely applied for imaging residual brain glioblastoma, colorectal cancer, and pleural malignancy [19–22]. However, only limited studies are available [23]. Apart from these probes, gGlu-HMRG is characterized by an activatable cancer-specific fluorescence probe targeting GGT that enables rapid and sensitive visualization of cancer cells with topical application when cancer cells have sufficient GGT expression.

This study is the first investigation for lung cancer imaging less than 1 mm using gGlu-HMRG for the purpose of intraoperative imaging. Unfortunately, sensitivity and specificity of lung cancer imaging with gGlu-HMRG in our *ex vivo* experiment study were limited to 43.8% and 84.9%, respectively. Hanigan et al. demonstrated that 18 adenocarcinomas of 44 cases of lung cancer (40.9%) had high GGT expression, evidenced by immunohistochemical staining, which added support to our results [11]. Although sensitivity was as low as about 50%, selecting the lung cancer cases especially for females, never-smokers, and cases with adenocarcinoma, sensitivity and specificity were raised up to 78.9% and 73.7%, respectively. And more, if we will be able to confirm the availability of gGlu-HMRG using preoperative biopsy specimen of a lung cancer patient before operation, we could perform intraoperative lung cancer fluorescence imaging without fail. Sensitivity must be more improved to be nearly 90% to 100% when preoperative case selection is possible.

Clinically, intraoperative application of gGlu-HMRG may be feasible and advantageous for visualization of cancer cells, especially in surgical margin or pleural cavity of lung cancer surgery. Limited resection or wedge resection mainly by video-assisted thoracic surgery has been recently on the rise [24–26]. One of the issues is locoregional

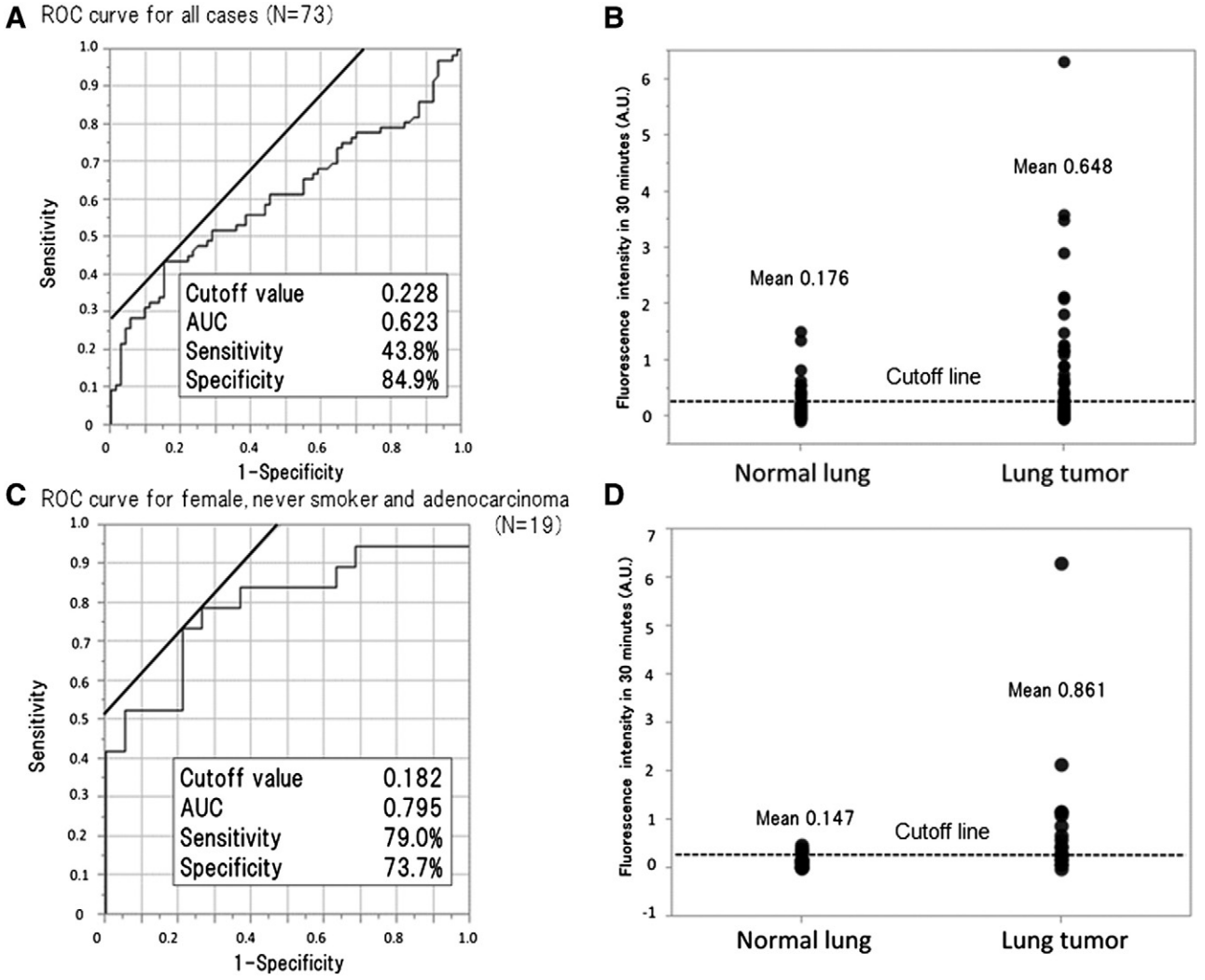

Figure 6. Increase in fluorescence intensity in lung tumor and normal lung after 30 minutes and the results of cutoff value, sensitivity, and specificity of gGlu-HMRG for detection of lung cancer analyzed by receiver operating characteristic curves for all 73 cases and a subset of 19 patients comprising females, never-smokers, and patients with adenocarcinoma. Sensitivity and specificity for all cases were 43.8% (32/73 cases) and 84.9% (62/73 cases), respectively. Limited to the 19 cases of females, never-smokers, and cases of adenocarcinoma, the sensitivity and specificity were 78.9% (15/19 cases) and 73.7% (14/19 cases), respectively. *AUC*, area under curve.

recurrence, which is increasing in near future. In previous reports, the rate of locoregional recurrence has ranged between 1.1% and 17.2% (median, 6.0%) [27–32]. And more, it is also challenging to detect very small foci of pleural dissemination or carcinomatous pleuritis that are macroscopically invisible [33]. In the current practical method, a pathological examination for a surgical margin or pleural lavage cytology is performed to detect a remnant tumor cell, taking around 30 minutes. However, a surgeon could not detect the exact location of a tumor cell intraoperatively. And even if five-aminolaevulinic acid is used for a lung cancer patient with high sensitivity, a tiny tumor within 1 mm in diameter could not be seen [23]. In contrast, intraoperative fluorescence imaging with gGlu-HMRG could be a simple and effective procedure to detect small foci of cancer cells within 1 mm in diameter in several minutes if a cancer cell has high GGT activity.

There are some limitations of gGlu-HMRG in practical use. Because the wavelength of HMRG is around 500 nm, superficially exposed cancer cells could be detected by fluorescence imaging with topical gGlu-HMRG. Meanwhile, deeply located cancer would not be visualized. It should also be mentioned that gGlu-HMRG was nonspecifically activated in some lungs, leading to a false-positive rate up to 15.1%. Because macrophages have some GGT activity [4], we considered that lung tissue with accumulation of histiocytes may have a possibility to exhibit increased fluorescence when exposed to gGlu-HMRG (e-Figure 2). Same results were ascertained in three cases including case 4. A cytotoxicity test and development of a medical device for fluorescence imaging are also indispensable for increasing the practical utility of gGlu-HMRG. Although several challenges remain, this rapidly activatable fluorescence probe could be of great value for general thoracic surgery.

Conclusions

We have validated the utility of gGlu-HMRG as an intraoperative rapid imaging tool. We believe that detecting pleural dissemination, small mediastinal lymph node metastasis, or other small foci of lung cancer cells should greatly help surgeons to improve the prognosis in near future.

Supplementary data to this article can be found online at http://dx.doi.org/10.1016/j.tranon.2016.03.007.

Acknowledgements

We are grateful to Prof. Kohei Miyazono, Graduate School of Medicine, The University of Tokyo, for research guidance in qRT-PCR and to Assoc. Prof. Rumi Hino, The Faculty of Sports and Health Science, Daito Bunka University, for research assistance of pathological diagnosis.

References

[1] Ministry of Health, Labour and Welfare (). Vital Statistics Japan. Available from http://www.mhlw.go.jp/english/database/db-hw/dl/81-1a2en.pdf . [accessed in 2014. Aug.21].

[2] Urano Y, Sakabe M, Kosaka N, Ogawa M, Mitsunaga M, Asanuma D, Kamiya M, Young MR, Nagano T, and Choyke PL, et al (2011). Rapid cancer detection by topically spraying a γ-glutamyltranspeptidase-activated fluorescent probe. *Sci Transl Med* **23**, 110–119.

[3] Heisterkamp N, Groffen J, Warburton D, and Sneddon TP (2008). The human gamma-glutamyltransferase gene family. *Hum Genet* **123**, 321–332.

[4] Hanigan MH and Frierson Jr HF (1996). Immunohistochemical detection of gamma-glutamyl transpeptidase in normal human tissue. *Histochem Cytochem* **44**, 1101–1108.

[5] Hanigan MH (1998). γ-Glutamyl transpeptidase, a glutathionase: its expression and function in carcinogenesis. *Chem Biol Interact* **111–112**, 333–342.

[6] Corti A, Franzini M, Paolicchi A, and Pompella A (2010). Gamma-glutamyltransferase of cancer cells at the crossroads of tumor progression, drug resistance and drug targeting. *Anticancer Res* **30**, 1169–1182.

[7] Pompella A, Corti A, Paolicchi A, Giommarelli C, and Zunino F (2007). Gamma-glutamyltransferase, redox regulation and cancer drug resistance. *Curr Opin Pharmacol* **7**, 360–366.

[8] Pankiv S, Møller S, Bjorkoy G, Moens U, and Huseby NE (1760). Radiation induced upregulation of gamma-glutamyltransferase in colon carcinoma cells is mediated through the Ras signal transduction pathway. *Biochim Biophys Acta* **2006**, 151–157.

[9] Braun L, Goyette M, Yaswen P, Thompson NL, and Fausto N (1987). Growth in culture and tumorigenicity after transfection with the ras oncogene of liver epithelial cells from carcinogen-treated rats. *Cancer Res* **47**, 4116–4124.

[10] Pompella A, De Tata V, Paolicchi A, and Zunino F (2006). Expression of gamma-glutamyltransferase in cancer cells and its significance in drug resistance. *Biochem Pharmacol* **71**, 231–238.

[11] Hanigan MH, Frierson Jr HF, Swanson PE, and De Young BR (1999). Altered expression of gamma-glutamyl transpeptidase in human tumors. *Hum Pathol* **30**, 300–305.

[12] Shibuya K, Komaki R, Shintani T, Itasaka S, Ryan A, Jürgensmeier JM, Milas L, Ang K, Herbst RS, and O'Reilly MS (2007). Targeted therapy against VEGFR and EGFR with ZD6474 enhances the therapeutic efficacy of irradiation in an orthotopic model of human non–small-cell lung cancer. *Int J Radiat Oncol Biol Phys* **69**, 1534–1543.

[13] Fushiki H, Kanoh-Azuma T, Katoh M, Kawabata K, Jiang J, Tsuchiya N, Satow A, Tamai Y, and Hayakawa Y (2009). Quantification of mouse pulmonary cancer models by microcomputed tomography imaging. *Cancer Sci* **100**, 1544–1549.

[14] Sobin LH, Gospodarowicz MK, and Wittekind C (2009). lung and pleural tumours. In: Sobin LH, Gospodarowicz MK, Wittekind C, editors. UICC International Union Against Cancer. , TNM Classification of Malignant Tumours, 7th ednOxford: Wiley-Blackwell; 2009. p. 138–146.

[15] Travis WD, Brambilla E, Müller-Hermelink HK, and Harris CC (2004). Pathology and Genetics of Tumours of the Lung, Pleura, Thymus and Heart. In: Travis WD, Brambilla E, Müller-Hermelink HK, Harris CC, editors. World Health Organization Classification of Tumours. Lyon: IARC Press; 2004. p. 9–124.

[16] Te Velde EA, Veerman T, Subramaniam V, and Ruers T (2010). The use of fluorescent dyes and probes in surgical oncology. *Eur J Surg Oncol* **36**, 6–15.

[17] Zhang H, Fan J, Wang J, Zhang S, Dou B, and Peng X (2013). An off-on COX-2-specific fluorescent probe: targeting the Golgi apparatus of cancer cells. *J Am Chem Soc* **135**, 11663–11669.

[18] Koyama Y, Hama Y, Urano Y, Nguyen DM, Choyke PL, and Kobayashi H (2007). Spectral fluorescence molecular imaging of lung metastases targeting HER2/neu. *Clin Cancer Res* **13**, 2936–2945.

[19] Zhao S, Wu J, Wang C, Liu H, Dong X, Shi C, Shi C, Liu Y, Teng L, and Han D, et al (2013). Intraoperative fluorescence-guided resection of high-grade malignant gliomas using 5-aminolevulinic acid-induced porphyrins: a systematic review and meta-analysis of prospective studies. *PLoS One* **8**e63682.

[20] Baas P, Triesscheijn M, Burgers S, van Pel R, Stewart F, and Aalders M (2006). Fluorescence detection of pleural malignancies using 5-aminolaevulinic acid. *Chest* **129**, 718–724.

[21] Kondo Y, Murayama Y, Konishi H, Morimura R, Komatsu S, Shiozaki A, Kuriu Y, Ikoma H, Kubota T, and Nakanishi M, et al (2014). Fluorescent detection of peritoneal metastasis in human colorectal cancer using 5-aminolevulinic acid. *Int J Oncol* **45**, 41–46.

[22] Ohgari Y, Nakayasu Y, Kitajima S, Sawamoto M, Mori H, Shimokawa O, Matsui H, and Taketani S (2005). Mechanisms involved in delta-aminolevulinic acid (ALA)-induced photosensitivity of tumor cells: relation of ferrochelatase and uptake of ALA to the accumulation of protoporphyrin. *Biochem Pharmacol* **71**, 42–49.

[23] Pikin O, Filonenko E, Mironenko D, Vursol D, and Amiraliev A (2012). Fluorescence thoracoscopy in the detection of pleural malignancy. *Eur J Cardiothorac Surg* **41**, 649–652.

[24] Leshnower BG, Miller DL, Fernandez FG, Pickens A, and Force SD (2010). Video-assisted thoracoscopic surgery segmentectomy: a safe and effective procedure. *Ann Thorac Surg* **89**, 1571–1576.

[25] Atkins BZ, Harpole Jr DH, Mangum JH, Toloza EM, D'Amico TA, and Burfeind Jr WR (2007). Pulmonary segmentectomy by thoracotomy or thoracoscopy: reduced hospital length of stay with a minimally-invasive approach. *Ann Thorac Surg* **84**, 1107–1112 [discussion 1112–3].

[26] Yano T, Yokoyama H, Yoshino I, Tayama K, Asoh H, Hata K, and Ichinose Y (1995). Results of a limited resection for compromised or poor-risk patients with clinical stage I non–small cell carcinoma of the lung. *J Am Coll Surg* **181**, 33–37.

[27] Ginsberg RJ and Rubinstein LV (1995). Randomized trial of lobectomy versus limited resection for T1 N0 non–small cell lung cancer. Lung Cancer Study Group. *Ann Thorac Surg* **60**, 615–622 [discussion 622–3].

[28] Martini N, Bains MS, Burt ME, Zakowski MF, McCormack P, Rusch VW, and Ginsberg RJ (1995). Incidence of local recurrence and second primary tumors in resected stage I lung cancer. *J Thorac Cardiovasc Surg* **109**, 120–129.

[29] Nomori H, Mori T, Ikeda K, Yoshimoto K, Iyama K, and Suzuki M (2012). Segmentectomy for selected cT1N0M0 non–small cell lung cancer: a prospective study at a single institute. *J Thorac Cardiovasc Surg* **144**, 87–93.

[30] Okada M, Koike T, Higashiyama M, Yamato Y, Kodama K, and Tsubota N (2006). Radical sublobar resection for small-sized non–small cell lung cancer: a multicenter study. *J Thorac Cardiovasc Surg* **132**, 769–775.

[31] Okada M, Mimae T, Tsutani Y, Nakayama H, Okumura S, Yoshimura M, and Miyata Y (2014). Segmentectomy versus lobectomy for clinical stage IA lung adenocarcinoma. *Ann Cardiothorac Surg* **3**, 153–159.

[32] El-Sherif A, Gooding WE, Santos R, Pettiford B, Ferson PF, Fernando HC, Urda SJ, Luketich JD, and Landreneau RJ (2006). Outcomes of sublobar resection versus lobectomy for stage I non–small cell lung cancer: a 13-year analysis. *Ann Thorac Surg* **82**, 408–415 [discussion 415–6].

[33] Ichinose Y, Tsuchiya R, Yasumitsu T, Koike T, Yamato Y, Nakagawa K, Tada H, Yokoi K, Nagai K, and Kase M, et al (2001). Prognosis of non–small cell lung cancer patients with positive pleural lavage cytology after a thoracotomy: results of the survey conducted by the Japan Clinical Oncology Group. *Lung Cancer* **31**, 37–41.